Exploring functional pairing between surface glycoconjugates and human galectins using programmable glycodendrimersomes

Qi Xiao[a], Anna-Kristin Ludwig[b], Cecilia Romanò[c], Irene Buzzacchera[a,d,e,f], Samuel E. Sherman[a], Maria Vetro[c], Sabine Vértesy[b], Herbert Kaltner[b], Ellen H. Reed[g], Martin Möller[d,e], Christopher J. Wilson[f], Daniel A. Hammer[g,h], Stefan Oscarson[c], Michael L. Klein[i,1], Hans-Joachim Gabius[b], and Virgil Percec[a,1]

[a]Roy & Diana Vagelos Laboratories, Department of Chemistry, University of Pennsylvania, Philadelphia, PA 19104-6323; [b]Institute of Physiological Chemistry, Faculty of Veterinary Medicine, Ludwig-Maximilians-University, 80539 Munich, Germany; [c]Centre for Synthesis and Chemical Biology, University College Dublin, Dublin 4, Ireland; [d]DWI – Leibniz Institute for Interactive Materials, RWTH Aachen University, 52074 Aachen, Germany; [e]Institute of Technical and Macromolecular Chemistry, RWTH Aachen University, 52074 Aachen, Germany; [f]NovioSense B.V., 6534 AT Nijmegen, The Netherlands; [g]Department of Bioengineering, University of Pennsylvania, Philadelphia, PA 19104-6321; [h]Department of Chemical and Biomolecular Engineering, University of Pennsylvania, Philadelphia, PA 19104-6391; and [i]Institute of Computational Molecular Science, Temple University, Philadelphia, PA 19122

Contributed by Michael L. Klein, January 4, 2018 (sent for review November 16, 2017; reviewed by Timothy J. Deming and Yoshiko Miura)

Precise translation of glycan-encoded information into cellular activity depends critically on highly specific functional pairing between glycans and their human lectin counter receptors. Sulfoglycolipids, such as sulfatides, are important glycolipid components of the biological membranes found in the nervous and immune systems. The optimal molecular and spatial design aspects of sulfated and nonsulfated glycans with high specificity for lectin-mediated bridging are unknown. To elucidate how different molecular and spatial aspects combine to ensure the high specificity of lectin-mediated bridging, a bottom-up toolbox is devised. To this end, negatively surface-charged glycodendrimersomes (GDSs), of different nanoscale dimensions, containing sulfo-lactose groups are self-assembled in buffer from a synthetic sulfatide mimic: Janus glycodendrimer (JGD) containing a 3′-*O*-sulfo-lactose headgroup. Also prepared for comparative analysis are GDSs with nonsulfated lactose, a common epitope of human membranes. These self-assembled GDSs are employed in aggregation assays with 15 galectins, comprising disease-related human galectins, and other natural and engineered variants from four families, having homodimeric, heterodimeric, and chimera architectures. There are pronounced differences in aggregation capacity between human homodimeric and heterodimeric galectins, and also with respect to their responsiveness to the charge of carbohydrate-derived ligand. Assays reveal strong differential impact of ligand surface charge and density, as well as lectin concentration and structure, on the extent of surface cross-linking. These findings demonstrate how synthetic JGD-headgroup tailoring teamed with protein engineering and network assays can help explain how molecular matchmaking operates in the cellular context of glycan and lectin complexity.

glycodendrimers | glycolipids | aggregation

The enormous potential of glycans of cellular glycoconjugates to serve as biological messengers has spurred efforts to map the glycome (1–4). In parallel, work with synthetic multivalent carbohydrates and neoglycoconjugates is revealing that topological features of glycan presentation on a scaffold such as protein, lipid, or microdomain come into play when these messages are "read" by endogenous receptors known as lectins (5–9). A similar situation likely obtains for the "readers." This complementarity ensures that the functional pairing, which is of broad physiological significance, especially for cell surface phenomena, achieves the desired specificity (10, 11). Cell adhesion and bridging often critically depend on glycan–lectin recognition, and stringent nonpromiscuous selection occurs when forming pairs despite the vast diversity of glycoconjugates, as, for example, with the C-type lectins and for the cell adhesion selectins (12, 13). However, the underlying structural parameters governing the selection process are not yet defined quantitatively. Confronted with the combination of natural glycan complexity and the result of evolutionary structure diversification within a lectin family, the ultimate experimental strategy would seem to require full glycome and lectin network analysis.

Although chemical control of glycoengineering of cells by inserting glycopolymers (14–22) into membranes was previously reported (23, 24), to date, much research in the field of glycan–lectin matchmaking has focused on answering the question posed decades ago, namely: Are glycan molecules in search of a function (25)? These experiments are making us aware that our understanding of the factors governing the high specificity of pairing glycoconjugates with lectins is still very limited (26, 27) despite its broad impact on cell physiology (28).

Accordingly, here we employ an approach based on model systems to begin to tackle this formidable problem. In essence, self-assembled nanovesicles having programmable surfaces presenting sugar moieties are used in combination with natural and engineered lectins to explore the complexity of glycan–lectin specificity. The nanovesicle toolbox comprises Janus glycodendrimers

Significance

Cells are decorated with charged and uncharged carbohydrate ligands known as glycans, which are responsible for several key functions, including their interactions with proteins known as lectins. Here, a platform consisting of synthetic nanoscale vesicles, known as glycodendrimersomes, which can be programmed with cell surface-like structural and topological complexity, is employed to dissect design aspects of glycan presentation, with specificity for lectin-mediated bridging. Aggregation assays reveal the extent of cross-linking of these biomimetic nanoscale vesicles—presenting both anionic and neutral ligands in a bioactive manner—with disease-related human and other galectins, thus offering the possibility of unraveling the nature of these fundamental interactions.

Author contributions: M.L.K., H.-J.G., and V.P. designed research; Q.X., A.-K.L., C.R., I.B., S.E.S., M.V., and E.H.R. performed research; M.V., S.V., M.M., C.J.W., D.A.H., and S.O. contributed new reagents/analytic tools; Q.X., I.B., S.E.S., H.K., S.O., M.L.K., H.-J.G., and V.P. analyzed data; and M.L.K., H.-J.G., and V.P. wrote the paper.

Reviewers: T.J.D., University of California, Los Angeles; and Y.M., Kyushu University.

The authors declare no conflict of interest.

See Commentary on page 2548.

[1]To whom correspondence may be addressed. Email: mlklein@temple.edu or percec@sas.upenn.edu.

This article contains supporting information online at www.pnas.org/lookup/suppl/doi:10.1073/pnas.1720055115/-/DCSupplemental.

Published online January 30, 2018.

(JGDs) with various sugar headgroups obtained by synthesis. JGD design enables control of glycan presentation/density and diversity, eventually mimicking structural and topological features encountered on cell surfaces. As proof-of-principle, the nanovesicle toolbox is employed to couple with adhesion/growth-regulatory galectins (Gals).

This family of lectins has been selected because of its potent bridging activity (29–31). Structurally, the lectins are grouped into the three categories shown in Fig. 1*A*, often present as a network in human tissues (32–35). In each case, i.e., the homodimer, the linker-associated heterodimer, and the chimera-type monomer capable of self-aggregation (Fig. 1*A*), the protein design enables nanovesicles–counterreceptor cross-linking. Since results of current research demonstrate that each family member appears to have its own activity profile with emerging cases of functional antagonism, cooperation, and redundancy, bridging activities are likely to differ and respond differently to features of ligand display. In principle, each is relevant to make functional pairing possible.

To test this hypothesis and gain insights into the mutual relationship of surface glycan presentation and galectin design, covering all three types shown in Fig. 1*A*, here we test four disease-related human galectins on nanoscale glycodendrimersomes (GDSs) (36, 37) that present the canonical ligand D-lactose (Lac) and its charged 3′-*O*–sulfated derivative. Starting with the synthesis of the activated 3′-*O*–sulfated lactose (suLac) derivative as headgroup of the self-assembling JGDs, we then report (*i*) the design, synthesis, and self-assembly of the first stable GDSs with negative surface charge, a common feature of cells; (*ii*) the impact of structural characteristics both of galectins, such as valency or linker length, and of GDSs, such as modulation of glycan density on GDS aggregation; and (*iii*) a comparative (network-style) analysis of wild-type (WT) Gal-1, Gal-3, Gal-4, and Gal-8. A natural variant and a hybrid protein, obtained by modular transplantation, as well as combinations of two bioactive ligands on the surface of the same GDSs plus mixtures of separate GDS preparations, purposefully broaden the experimental scope. These Lac and suLac-presenting GDSs mimic the surface of biological membranes containing natural sulfatides and galactocerebrosides (Fig. S1*A*) and are formed by the self-assembly of sequence-defined JGDs without the need of coassembly of glycolipids with phospholipids. Specifically, the GDSs (36, 37) are prepared by simple injection of JGDs in buffer. The aggregation of GDSs by galectins provides the most direct, simple, and convenient method to evaluate the *trans*-bridging by increased UV-vis turbidity (Fig. S1*B*). The *cis* activity of galectins is not accessible by this simple method since, unlike cell membranes, GDSs do not provide biosignals.

Results and Discussion

The Lectin Toolbox. The test panel represents the three natural types of design of human galectins, in general terms shown in Fig. 1*A*. In detail, it consists of a noncovalently associated homodimer (Gal-1; Fig. 1*B*), two cases of linker-connected heterodimer (Gal-4 in Fig. 1*C*, and Gal-8 in Fig. 1*D*) and the chimera-type Gal-3 (Fig. 1*E*). It is built from the C-terminal carbohydrate recognition domain (CRD) and an N-terminal tail (NT) with nine nontriple helical collagenous repeats responsible for self-association in the presence of suited ligands and a peptide with two sites for serine phosphorylation (Fig. 1*E*) (38). In addition, to deliberately expand examination of structure–activity relationships, we added five proteins with distinct structural change: an engineered homotetramer of human Gal-1, i.e., $(Gal\text{-}1)_4$, two variants of Gal-4 with reduced linker length, i.e., Gal-4V/P, the single-nucleotide polymorphism (SNP)-based F19Y Gal-8 protein, and a Gal-3 variant obtained by transplanting the N-terminal CRD of Gal-8 (Gal-8N) to Gal-3's NT, i.e., Gal-3NT/8N (Fig. 1*E*). Comparative analysis of the three types of design of human galectins including assessment of impact of linker length and mode of CRD presentation is thus possible.

The four disease-related human galectins employed share binding properties with the canonical ligand Lac. To reveal whether and how their bridging capacity is modulated by the

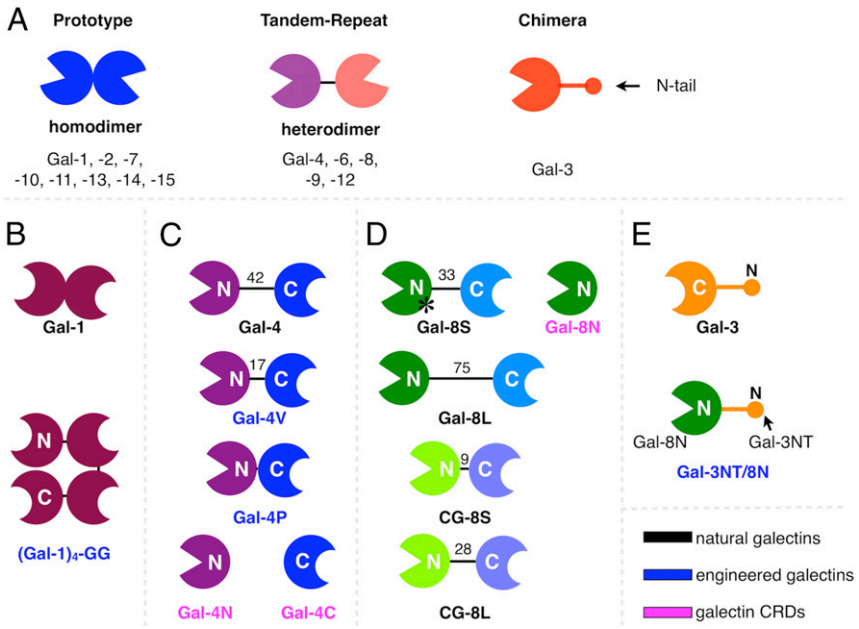

Fig. 1. Modular architectures of vertebrate galectins (*A*) including prototype, tandem-repeat, and monomeric chimera-type proteins. Illustration of the natural forms of Gal-1 (*B*), Gal-4 (*C*), Gal-8 (*D*), and Gal-3 (*E*), as well as engineered variants and the separate CRDs derived from in situ proteolytic cleavage. N and C indicate type of CRD positioning relative to the termini. Numbers indicate length (amino acid, AA) of linkers between CRDs, while * denotes the site of the sequence deviation in the human SNP variant protein F19Y.

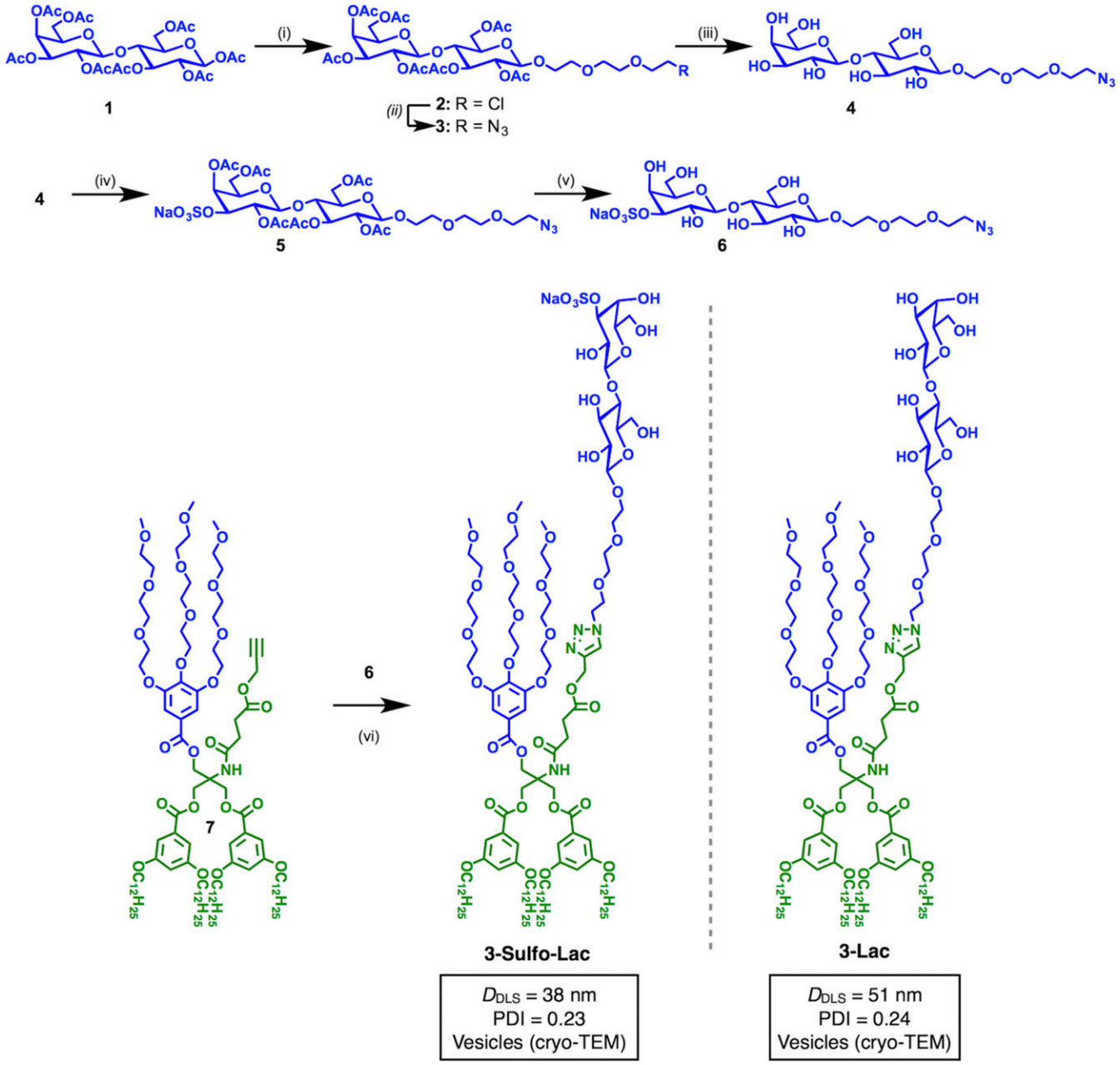

Fig. 2. Synthesis of JGD **3-Sulfo-Lac** with 3′-*O*-sulfo-D-lactose (suLac) headgroup, and the chemical structure of **3-Lac** with D-lactose (Lac) headgroup. Reagents and conditions: (*i*) 2-(2-(2-chloroethoxy)ethoxy)ethanol, $BF_3{\cdot}Et_2O$, CH_2Cl_2, 0 °C to 23 °C, 15 h, 80%; (*ii*) NaN_3, DMF, 80 °C, 15 h, 74%; (*iii*) MeONa, MeOH, pH = 10, 23 °C, 7 h, 95%; (*iv*) Bu_2SnO, dry MeOH, 60 °C, 3 h; $SO_3{\cdot}NMe_3$, 1,4-dioxane, 23 °C, 48 h; and Ac_2O, pyridine, 23 °C, 15 h, 65%; (*v*) MeONa, MeOH, pH = 12, 23 °C, 10 h, 91%; (*vi*) $CuSO_4{\cdot}5H_2O$, sodium ascorbate, THF, water, 23 °C, 24 h, 55%. The diameter (D_{DLS}) and polydispersity index (PDI) were determined by DLS at 0.1 mM of sugar in PBS (PBS 1×, pH 7.4).

presence of a ligand with more discriminatory ability than Lac, we selected its charged 3′-*O*−sulfated form suLac for this study. SuLac is a strong binder to Gal-1 (39–41) and Gal-3 (40, 42, 43), and their association with cellular glycoconjugates seen in tissue sections is competitively blocked efficiently by this disaccharide (44). Although heterodimeric design is shared by Gal-4 and Gal-8, both suLac receptors as full-length proteins, sequence disparities account for differences: The two Gal-4 CRDs are binders (45–48), whereas the affinity gap between the two CRDs of Gal-8 ranges from high (nanomolar) affinity between Gal-8N and suLac to very low activity for Gal-8C (43, 48–52). Of note, the two CRDs of Gal-8 also differ widely, i.e., about 5- to 10-fold, in affinity to Lac (49, 52, 53), measured in the case of the full-length protein by NMR titrations at 128 ± 9 μM (Gal-8N), similar, to, e.g., Gal-1, and 1,478 ± 69 μM (Gal-8C) (53). Consequently, Gal-8C's purification was not possible by affinity chromatography on resin-presenting Lac but required fusion protein technology. Working under the same conditions with Gal-1 vs. Gal-4 and Gal-8 enables comparison of homodimers and heterodimers, and experiments with Gal-4 and Gal-8 probe into intragroup differences (for details on Gal-3, see *The Case of Chimera-Type Gal-3*). To test how structure and affinity affect GDS aggregation, surface programming required synthesis of the suLac headgroup that can be conjugated to a JGD.

The Sugar Headgroup Toolbox. Janus dendrimers containing both hydrophilic and hydrophobic dendrons, self-assembled into vesicles denoted dendrimersomes, provide a versatile platform to mimic biological membranes (36, 54–58). GDSs assembled from JGDs with sugar on their hydrophilic dendrons, and sequence-defined density of sugars, provided tools that have been established for various types of sugar–lectin recognition (36, 37, 59–65). The synthesis of the azidoethylene glycol spacer-equipped Lac derivative **3** was modified from our previous procedure (36), as outlined in Fig. 2. Commercially available 2-(2-(2-chloroethoxy) ethoxy)ethanol was used as aglycone instead of the corresponding tosylated compound, which doubled the yield in the reaction with peracetylated Lac **1** to give **2** (80% compared with 40%). Azide substitution of the chloride using NaN_3 in dimethylformamide (DMF) (leading to **3**, 74%) was followed by standard Zemplèn deacetylation affording **4** in 95% yield. To introduce the sulfate group at the 3′-OH, a direct tin-mediated regioselective sulfation (66) of unprotected **2** was preferred to one involving multistep protecting-group manipulations to generate a free 3′-OH followed by sulfation. Compound **4** was treated with Bu_2SnO in MeOH and then sulfated using a $SO_3{\cdot}NMe_3$ complex in dioxane to give the 3′-*O*–sulfated product. The crude compound was acetylated before silica gel column chromatography to afford **5** in an overall 65% yield from **4**. Final Zemplèn deacetylation yielded the target **6** without any further purification being required. The twin-mixed type JGD **3-Sulfo-Lac** (for NMR spectra, see Figs. S2 and S3) was synthesized by copper-catalyzed click chemistry with the alkyne-functionalized Janus dendrimer **7** and azide functionalized 3′-*O*-sulfated lactose **6** (55% yield). The twin-mixed Lac-containing JGD (**3-Lac**) was assembled into the corresponding GDS as reported previously (60–63), to investigate the properties of GDSs containing an anionic sugar headgroup.

Morphological Analysis of suLac-Presenting GDSs. JGD with suLac as ligand yield GDSs with anionic surface charges. GDSs with the suLac headgroups have features resembling those of Lac-presenting GDSs (59, 63), as exemplified by cryogenic transmission electron microscopy (cryo-TEM) images (Fig. S4). Vesicle diameter (38 nm vs. 51 nm) and polydispersity (at 0.23 vs. 0.24 for Lac-presenting GDSs) underscore this conclusion (Fig. 2). Given this similarity, the comparative activity assays will likely not be drastically affected by a morphological parameter on this level. To probe the spatial accessibility and bioactivity of this type of sugar headgroup, aggregation assays with the galectins were systematically performed.

Galectin-Dependent GDS Aggregation.

Comparison and effect of linker length. Measurements were carried out at the same mass concentration, which in these cases [except for $(Gal\text{-}1)_4$] of similar molecular weights results in molar concentrations within a rather small range. Although 3′-*O* sulfation formally increased the inhibitory activity of *N*-acetyllactosamine (LacNAc) on Gal-1–dependent hemagglutination about threefold (39), the presence of suLac on the GDS surface conferred no relative increase in OD readings (Fig. 3*A*). In fact, GDS aggregation of the suLac/Gal-1 pair was slower and reached a lower plateau level than for the Lac/Gal-1 combination. Covalent CRD connection and domain shuffling are means to produce variants with increased valency. By turning the homodimer into a covalently linked homotetramer (62) and testing this variant at the same mass concentration, increases of both parameters were obtained (Fig. 3*B*). Notably, both types of GDS preparations now reached equal plateau levels (Fig. 3*B*). However, the capacity to mediate firm aggregation cannot be predicted from measurements of binding (inhibitory) activity and depends on the quaternary structure of a prototype galectin.

Gal-4 is known as an adherens junction protein and bifunctional cargo binder in routed apical and neuronal transport of glycoproteins

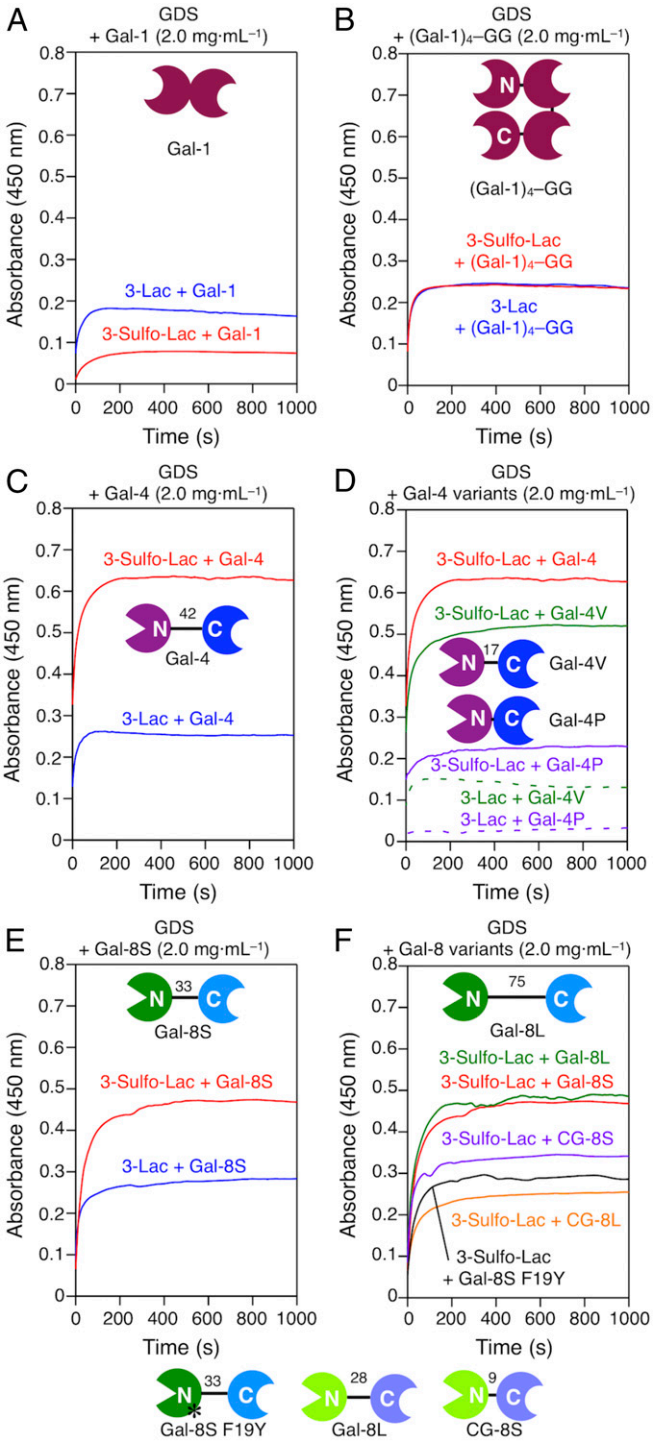

Fig. 3. Aggregation of GDSs self-assembled from **3-Sulfo-Lac** or **3-Lac** (0.1 mM, 900 μL) with galectins Gal-1 (*A*), $(Gal\text{-}1)_4$–GG (*B*), Gal-4 (*C*), Gal-4 variants (*D*), Gal-8S (*E*), and Gal-8 variants (*F*) (2 mg·mL^{-1}, 100 μL) in PBS (pH 7.4). * denotes the human SNP variant protein F19Y.

such as NCAM L1 as well as stabilizer of superrafts by binding sulfatides and LacNAc termini of complex-type N-glycans (67–71). The increased binding affinity to Lac with 3′O sulfation translates into a pronounced activity enhancement in the aggregation assay in this case (Fig. 3*C*). To study the effect of linker length on this activity, we compared the WT protein with two variants, in which we artificially shortened the linker as shown in Fig. 1*C*. Of note, the structures of the

CRDs are not affected by this engineering. The alteration of linker length had a significant effect, i.e., reduction of aggregation, which is strongest with the heterodimeric protein of minimal linker length (Fig. 3*D*). Gal-4, in contrast to Gal-8 (see below), has no natural linker-length variant, and, due to alternative splicing, does not simply act as a bivalent protein. Conversely, Fig. 3*D* reveals a significant impact of linker length on aggregation activity. This section of Gal-4 is thus a major factor in determining the protein's function. This insight directs interest to further study inter-CRD communication and relative aspects of CRD presentation in the absence and presence of ligands experimentally (72–74). Interestingly, the linker sequences of the heterodimeric (tandem-repeat-type) galectins show no signs of homology, in contrast to their CRDs (34), so that the impact of linker presence and length may or may not be similar. The comparative measurements with Gal-8 will provide a first answer to this question.

Human Gal-8, first described as prostate carcinoma tumor antigen-1 (75), that mediates aggregation of such malignant cells to prevent anoikis (76) is a matricellular and bridging protein with a broad range of regulatory activities on immune and other cells (77–80). As seen for Gal-4 due to increased affinity by the 3′-*O* sulfation (Fig. 3*A*), aggregation with the physiologically most widely encountered form, i.e., Gal-8S (Fig. 1*D*) proceeds faster and reaches a higher plateau level for this ligand than for Lac (Fig. 3*E*). The two forms of human Gal-8 originating from alternative splicing, i.e., Gal-8S/L (Fig. 1*D*), however, maintain similar activity (Fig. 3*F*). In this case, the two different linker lengths do not markedly change this activity. Occurrence of linker-length variation in the chicken Gal-8 orthologs, which have shorter lengths (28 and 9 amino acids; see Fig. 1*D*) (81), enables the testing of natural Gal-8 proteins with a shorter linker than for human Gal-8S. Experimentally, the outcome is different from Gal-4 and the human Gal-8 proteins: In this case, the activity is negatively correlated with linker length (Fig. 3*F*). Finally, the SNP-based variant, whose presence in the population is associated with autoimmune diseases (82, 83), is less active than the WT protein (Fig. 3*F*). Since sulfated LaNAc I/II derivatives precluded Gal-8 binding to B cells, where Gal-1 and Gal-8 promote plasma cell formation (78), the decrease in GDS bridging may be related to impairment of cross-linking capacity by the seemingly subtle SNP-based F19Y substitution, as noted before with Lac-presenting GDSs (61).

These results document pronounced differences in aggregation capacity between human homodimeric/heterodimeric galectins, and also with respect to their responsiveness to a change of the ligand. Of note, the linker length can have an obviously differential effect, depending on the galectin type and origin. The linker evidently does not simply connect two CRDs but has importance beyond holding different CRDs together. Fittingly, in the case of Gal-8, placing six glycines between the two CRDs instead of the natural linker led to a partial loss of the typical proadhesive and antiadhesive properties (84).

Turning to a fundamental mode of regulation of cellular activities, orchestrated changes in lectin and counterreceptor availability have been detected, e.g., in galectin-mediated growth control of activated effector T cells (85) or pancreas carcinoma cells reexpressing the tumor suppressor $p16^{INK4a}$ (86), prompting us to perform a series of experiments by altering both lectin concentration and surface density of the ligand.

Effect of lectin concentration and surface density of ligand. Tested with Gal-4, the turbidity to reach a clearly strong signal required a lectin concentration of 0.5 mg·mL^{-1}, and then linear increases ensued up to plateau level (Fig. 4*A*). Covalent connection between the domains N and C (Fig. 4*A*) is essential to generate aggregation activity (see Gal-4N and Gal-4C in Fig. 4*B*). Gal-8 was less active at low concentrations, requiring a higher threshold than Gal-4 for a signal (Fig. 4*C*). The same qualitative grading was seen for the SNP-based variant. The N-terminal domain Gal-8N of Gal-8 is special, apparently capable of self-association, as dimer trapping by chemical cross-linking indicated (50). In line with results of respective cell assays (adhesion, activation) (84, 87), the Gal-8N CRD alone became a GDS agglutinin at concentration above 2 mg·mL^{-1} (Fig. 4*D*). Again, our experimental setup unveils highly relevant differences for their bioactivity profile between galectins of the same group. In other words, homologous proteins of the same design have their own characteristic activity profiles. Following measurements with different galectin concentrations, we next varied the surface availability of the ligand.

The density of bioactive ligand was varied by adding a JGD with an inert sugar headgroup, i.e., D-mannose (Man) (59, 64, 65), to the solution with suLac JGD in increasing amount. As observed in Fig. 5 *A* and *B*, no signal was obtained with the Man-presenting GDSs, excluding signal generation by a noncognate sugar or linker. Tested at the same galectin concentration, the sensitivities of Gal-4 and Gal-8 differ widely with respect to ligand density: Gal-8 is a much more potent sensor of suLac presence than Gal-4 (Fig. 5 *A* and *B*). Physiologically, the two galectins will thus react differently with cells, when ligand density is dynamically regulated. Revealing this switch-like behavior illustrates the strength of this fully programmable test platform. In the presence of both bioactive ligands, i.e., Lac and suLac, the

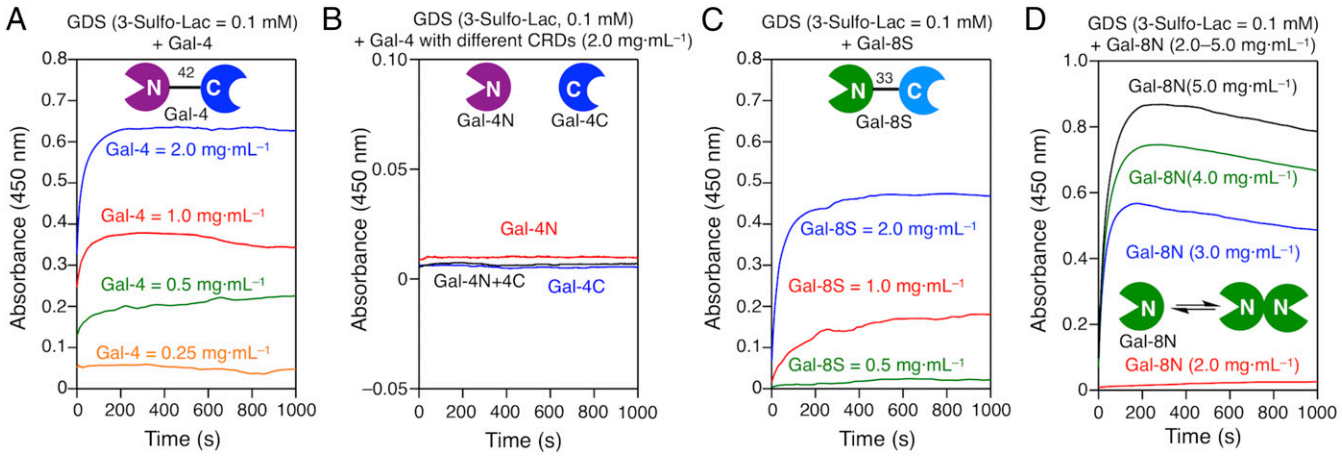

Fig. 4. Aggregation of GDSs (**3-Sulfo-Lac** = 0.1 mM, 900 μL) self-assembled with Gal-4 (*A*) and Gal-8S (*C*), tested at concentrations from 0.25 mg·mL^{-1} to 2 mg·mL^{-1}; CRDs of Gal-4 (*B*): Gal-4N, Gal-4C (2 mg·mL^{-1}, 100 μL), or 1:1 mixed Gal-4N/4C (1 mg·mL^{-1} of each domain, 100 μL); and N-CRD of Gal-8: Gal-8N (*D*) tested from 2 mg·mL^{-1} to 5 mg·mL^{-1} in PBS (pH 7.4).

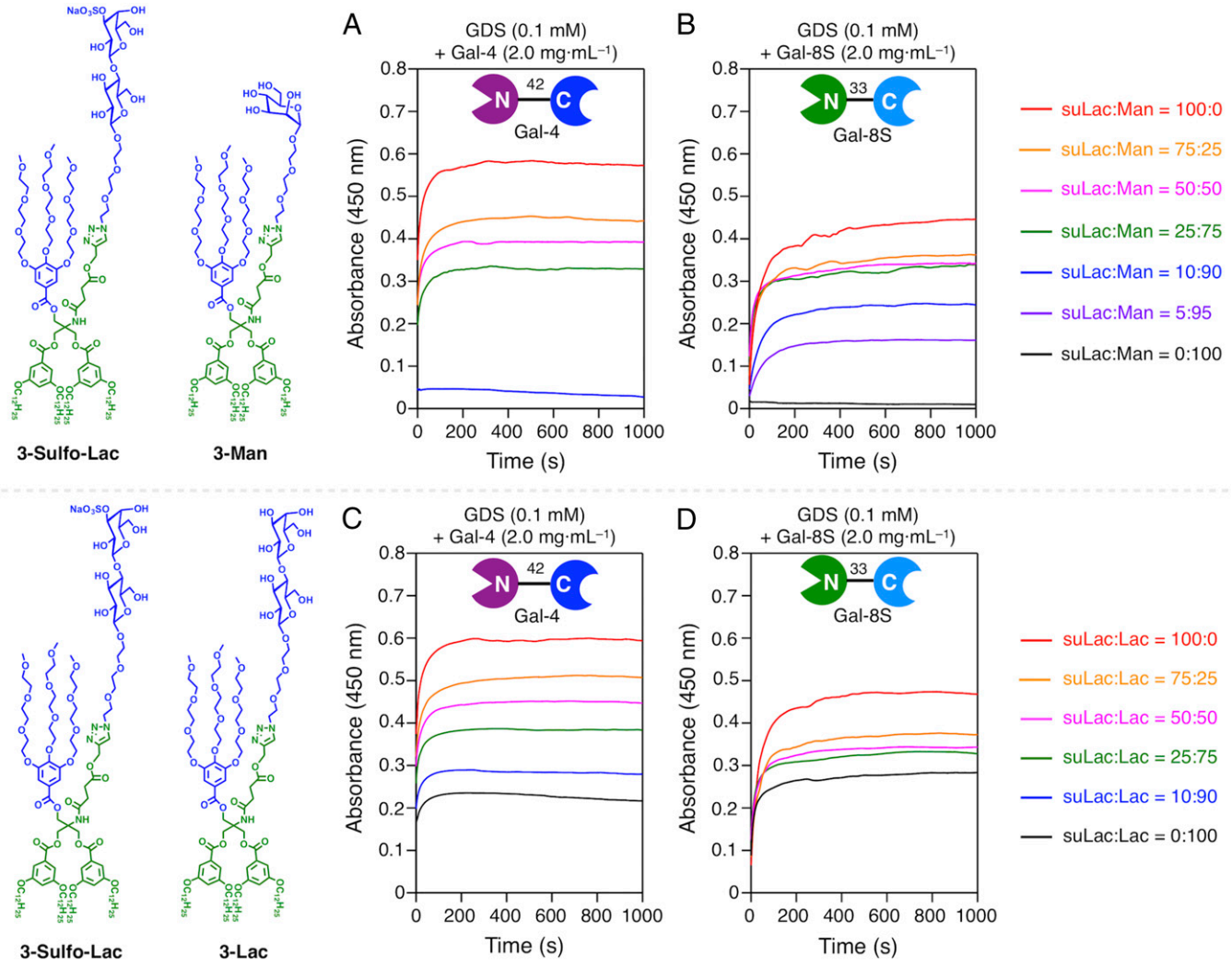

Fig. 5. Aggregation of GDSs coassembled from **3-Sulfo-Lac** and **3-Man** (59, 64, 65) (*Upper Left*) (suLac + Man = 0.1 mM, 900 μL) with Gal-4 (*A*) and Gal-8S (*B*) (2 mg·mL^{-1}, 100 μL), and GDSs coassembled from **3-Sulfo-Lac** and **3-Lac** (*Lower Left*) (suLac + Lac = 0.1 mM, 900 μL) with Gal-4 (*C*) and Gal-8S (*D*) (2 mg·mL^{-1}, 100 μL) in PBS (pH 7.4).

signal increase proceeds in a rather linear manner for Gal-4 and Gal-8S up to the plateau level (Fig. 5 *C* and *D* and Fig. S5).

When two bioactive ligands are presented not on the same GDS but as two GDS preparations in a mixture, then Gal-4 presence evokes an algebraically additive signal increase (Fig. 6*A*). It apparently reflects its functional bivalency to connect sulfatide and LacNAc-presenting N-glycans stoichiometrically. In the case of Gal-8, signal intensity was below this expectation (Fig. 6*B*). Probably, Gal-8C's rather low affinity to Lac, referred to *The Lectin Toolbox*, very strongly increased by presence of LacNAc repeats (51), comes into play here, intimating a level of selectivity by confining the ligand profile between CRDs. This finding directs efforts to further surface programming with respective structures. Testing that the level of physiological abundance of LacNAc repeats has switch-like properties thus becomes possible, an indication that our system enables versatile extensions to networks. In vivo, as glycans do, galectins often occur as a network so that assays in mixtures, as done for the binary glycan combinations, are a step required to simulate this situation.

The network aspect for dimeric proteins. In this series of experiments, the same JGD concentration was applied for assays at 1.0 mg·mL^{-1} for two dimeric galectins in separate assays and a mixture with this concentration. In each binary mixture, the signal was less than the algebraically additive value (Fig. 6 *C*–*E*). It thus appears that galectins in mixtures may stabilize already-forming/formed aggregates instead of forming a larger number of aggregates. A special case of mixture testing is Gal-8N. It becomes available to cells by thrombin cleavage of Gal-8L (88). When added in a nonaggregating concentration (Fig. 4*D*), its presence increases the readout, with Gal-4 slightly (Fig. 6*F*), and with Gal-8 strongly (Fig. 6*E*). Considering dynamic protein diversity by proteolytic cleavage, the outcome analysis of network behavior of dimeric galectins thus benefits from using a supramolecular model. In a network, the chimera-type Gal-3 will also play a role despite its fundamentally different design (Fig. 1*A*), and this has conspicuous biomedical relevance, for example, in driving osteoarthritis pathogenesis (89, 90).

The case of chimera-type Gal-3. This galectin, in line with previous experiments in hemagglutination and Lac-dependent GDS aggregation (36), is a weak agglutinin (Fig. 6*H*). Its binding to Lac-presenting GDSs is revealed by its ability to act as competitive inhibitor for Gal-1–dependent GDS aggregation (Fig. S6), an activity known from tumor cell growth regulation (91, 92). Since Gal-3 association with synthetic glycoclusters and polyvalent cell surface ligands can initiate its self-aggregation (38, 93) depending on the length of NT and even leading to bridging of two different counterreceptors, e.g., MUC16(CA125) and EGFR/β_1-integrin (93–95), the nature of the ligand(s) appears to modulate

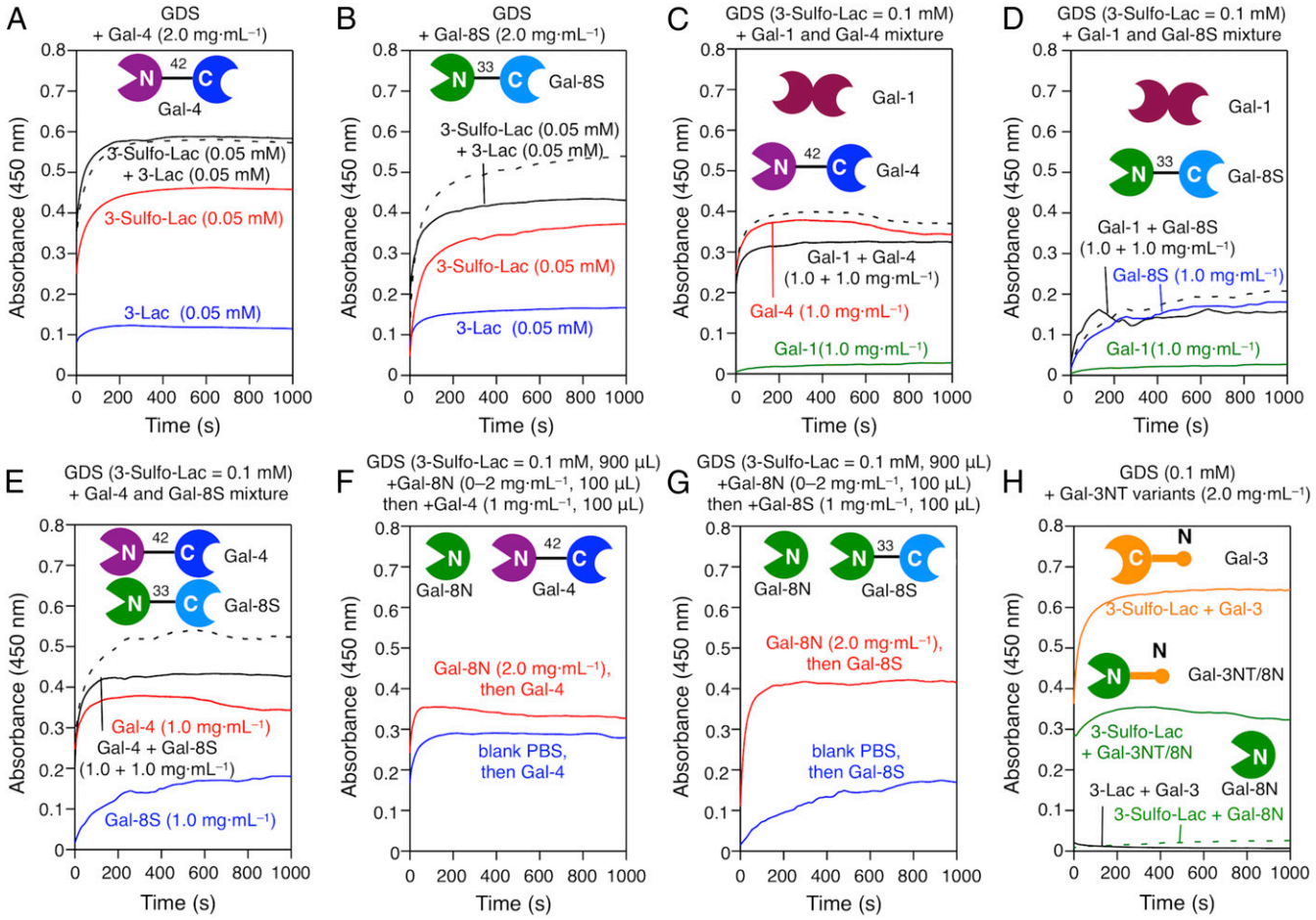

Fig. 6. Aggregation (*A* and *B*) (black solid lines) of mixed GDSs (900 µL) of both **3-Sulfo-Lac** (0.1 mM) and **3-Lac** (0.1 mM) to reach a final concentration **3-Sulfo-Lac** (0.05 mM) and **3-Lac** (0.05 mM) with Gal-4 (*A*) and Gal-8S (*B*) (2 mg·mL^{-1}, 100 µL) in PBS (pH 7.4). Aggregation (*C*–*E*) of GDSs with **3-Sulfo-Lac** (0.05 mM, red lines), **3-Lac** (0.05 mM, blue lines), and the sum curves (black dashed lines) of **3-Sulfo-Lac** (0.05 mM) and **3-Lac** (0.05 mM) were also indicated. Aggregation of GDSs (0.1 mM of **3-Sulfo-Lac**, 900 µL) with mixed galectins (100 µL) of Gal-1 + Gal-4 (*C*), Gal-1 + Gal-4 (*D*), and Gal-4 + Gal-8S (*E*) with 1:1 ratio in PBS (pH 7.4). The aggregation (*F* and *G*) of GDS from **3-Sulfo-Lac** with Gal-1 (green), Gal-4 (red), and Gal-8S (blue) (100 µL) at 1.0 mg·mL^{-1}. The sum curve (black dashed lines) of the combination of two relevant galectins was also indicated in each assay. Aggregation of GDSs (0.1 mM of **3-Sulfo-Lac**, 900 µL) with incubation with Gal-8N (0 mg·mL^{-1} to 2 mg·mL^{-1}, 100 µL) for 2 min, then Gal-4 (*F*) or Gal-8S (*G*) (1 mg·mL^{-1}, 100 µL) was added. Aggregation (*H*) of GDSs with Gal-3, Gal-3NT/8N, and Gal-8N (2.0 mg·mL^{-1}, 900 µL) in PBS (pH 7.4).

this aspect of lectin activity. We first asked the question whether this type of protein design is capable of strong aggregation, when the CRD's affinity to the ligand is higher than that of the Gal-3/Lac interaction. Coupling, by modular transplantation, the strong affinity of Gal-8N for suLac with the ability of Gal-3's NT for self-aggregation, to engineer a Gal-3NT/8N hybrid (Fig. 1*E*), led to a response on the OD reading of the monomeric variant protein similar to those obtained with (dimeric) Gal-8 (Figs. 3*E* and 6*H*). Gal-8N is in a nonaggregating concentration (Fig. 4*D* and 6*H*) without the help of NT. We then tested WT Gal-3, with the expectation of an activity similar to that of Gal-1 or lower. Although Gal-3 has lower affinity to suLac compared with Gal-8N, sulfate presence increased affinity relative to Lac, with factors of enhancement comparable to Gal-1 and Gal-4 (39, 42, 96), aggregation of suLac-presenting GDSs by WT Gal-3 reached a considerably higher plateau level than with the Gal-3NT/8N hybrid (Fig. 6*H*). A ligand-dependent increase in capacity for self-association of Gal-3 via the CRD, likely with a contribution by the NT (97–99), may underlie this steeply elevated signal. Accordingly, the presence of a sulfate group in the ligand, and the mixed CRD in protein design, has a tremendous activation potential. This finding underlines the merit of this experimental setup.

GDS Size–Aggregation Correlation. The sizes of GDSs employed in the present study were slightly different, 38 nm for **3-Sulfo-Lac** and 51 nm for **3-Lac** as obtained by self-assembly of their 0.1 mM solution of JGDs. Considering the potential effect of GDS size, aggregation assays with Gal-4 were also tested at 0.05 mM and 0.2 mM concentrations of JGDs (Fig. S7 *A* and *B*). Gal-4 was employed with the same stoichiometric ratio as that of the JGDs. The diameters of GDSs are known to be larger at higher JGD concentration (Fig. S7*C*) (63–65). Their relative aggregation ability can be quantified by the molar attenuation coefficient ε (Fig. S7*C*). For suLac GDSs, the value of ε is almost constant (see red columns in Fig. S7*C*). For Lac GDSs, larger GDSs exhibit higher ε (see blue columns in Fig. S7*C*). In all cases, the suLac GDSs showed much higher ε values than Lac GDSs. This trend enhances the conclusion based on the data discussed in Fig. 3*C*. When comparing both GDSs at identical diameters (44 nm for Lac GDSs at 0.05 mM of **3-Lac**, and 47 nm for suLac GDSs at 0.2 mM of **3-Sulfo-Lac**), suLac is about 4 times higher than Lac, based on their ε values. These data illustrate the

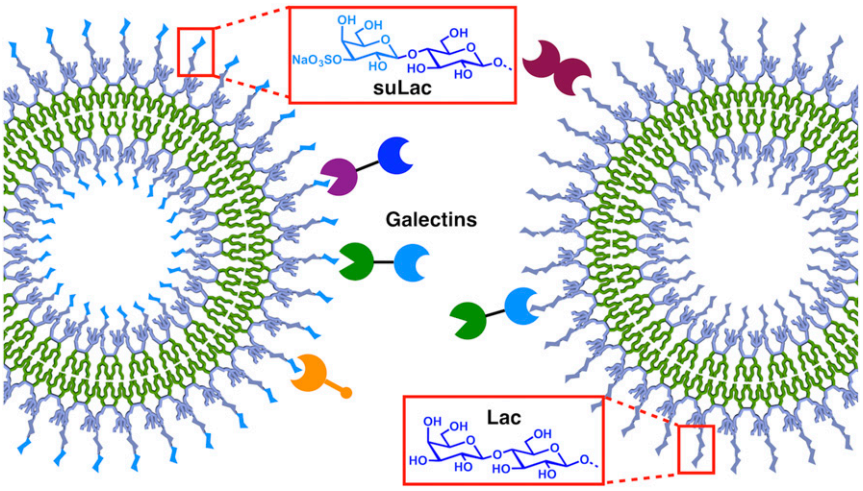

Fig. 7. Illustration of GDSs self-assembled from JGDs with Lac or suLac headgroups and selective binding with homodimeric, heterodimeric, and chimera-type human galectins.

response of glycan–lectin functional pairing to different surface curvatures.

The surface programming of nanoscale GDSs with Lac and negatively charged suLac, coupled with network testing of four families of natural and rationally engineered homodimeric, heterodimeric, and chimera-type human lectins, was elaborated to understand the specificity of pairing selected glycoconjugates with lectins (Fig. 7). Notably, the isoelectric points (pI values) of these galectins range from about 5.2 (Gal-1) to almost 9 for Gal-3 and Gal-8N. Therefore, it may be that the negative suLac-presenting GDSs bind more strongly with Gal-3 and Gal-8N than with Gal-1, due to the net positive charges of Gal-3 and Gal-8N at neutral pH (7.4 in PBS). If ionic/electrostatic interactions dominate the recognition, noncognate anionic ligands such as α2,6-sialylated N-glycans will be recognized by these galectins. However, such interactions were not found (39, 40, 43, 51, 52). More relevant, these galectins did not show nonspecific cell surface binding to the negative (GD1a) surface, instead requiring the presence of ganglioside GM1 and its presentation in microdomains (45, 49, 72, 83–85, 91). TLC plate assays with gangliosides for Gal-8 underline this conclusion (45, 49). In fact, X-ray analyses on Gal-4 and Gal-8 have demonstrated that electrostatic recognition occurs only when the anionic charge is present at a specific position (3′-OH) (47, 48, 83, 96). The exquisite specificity of the tested galectins to glycan, excluding binding by simple ionic interactions, guides recognition of cognate structures to lead to vesicle bridging. A graphical summary of the aggregation data at the described experimental conditions underscores both galectin-type and linker-length–dependent differences (Fig. 8). Most notably, Gal-3 becomes highly active, when the GDS surface presents suLac, a molecular switch (Fig. 8*D*). This result underscores the enormous potential of our approach.

Conclusion

The present experiments are able to unveil some of the key factors involved in this orthogonal relationship (100). Noncovalent homodimeric Gal-1 prefers to aggregate Lac-presenting GDSs, while covalently linked heterodimeric Gal-4 and Gal-8 prefer suLac-presenting GDSs. Shortening the linker length reduced the activity of Gal-4. Changing the linker length for two natural human Gal-8 variants showed less impact, but a single mutation on CRD lowered the activity dramatically (Fig. 3). Gal-4 has higher activity at low lectin concentration than Gal-8S (Fig. 4), while Gal-4 needs a higher sugar threshold on the GDS surface (Fig. 5). The different affinity of two domains on heterodimers is also demonstrated, especially on the N-CRD Gal-8N by a combination of GDS mixtures and lectin mixtures (Fig. 6 *A*–*G*). Connecting Gal-8N with the NT from chimera-type Gal-3 combined the affinity to suLac of the CRD and the aggregation ability of the NT to form oligomers (Fig. 6*H*).

The simple aggregation experiments reported here provided the most direct evidence of lectin/glycan-dependent affinity to the biorelevant *trans*-bridging between cell membranes. This bottom-up approach to the elucidation of the structure and function of the glycan of biological membranes is complementary

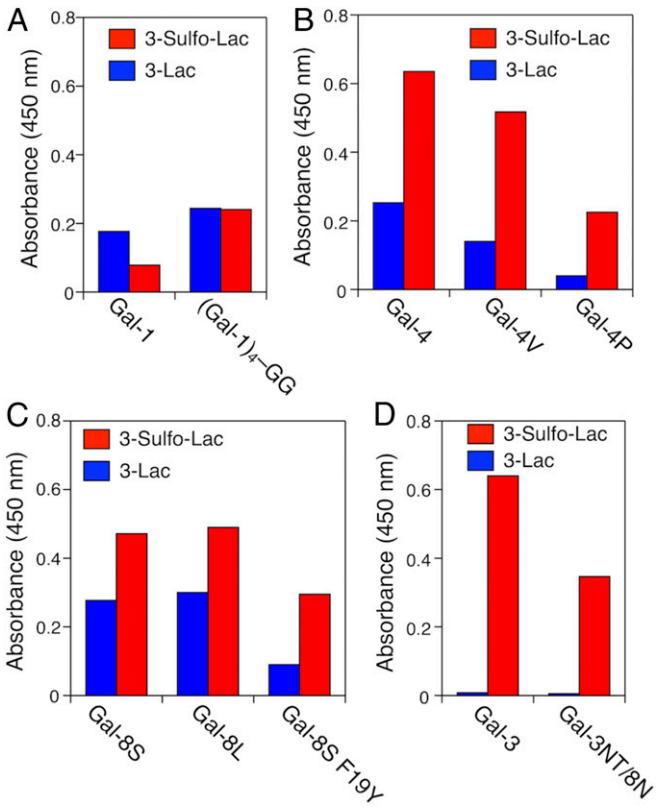

Fig. 8. Summary of aggregation assay data using GDSs self-assembled from **3-Sulfo-Lac** or **3-Lac** with Gal-1 (*A*), Gal-4 (*B*), Gal-8 (*C*), and Gal-3 (*D*) and respective variant proteins.

to the top-down efforts to map the glycan structurally (3, 4, 101). Going forward, further unveiling the key to functional pairing is likely to make innovative gain-of-function tools available. Eventually, they might be used, for example, to specifically scavenge a lectin at sites of clinically harmful activity or target the nanoparticles to lectins in vivo. Such routing has been surmised to be operative in a siglec-mediated internalization of mesenchymal stem cell-derived exosomes presenting appropriate sialoglycoconjugates by antigen-presenting cells in mice (102). Moreover, extracellular vesicles are also known to present α2,3-sialylated N-glycans and polyLacNAc repeats suited for homing to galectins (103, 104). Such events are likely to be amplified at the transition of the cell membrane surface from lamellar to cubic (65) when glycan–lectin pairing by modular membrane topologies combined with the experiments reported here is likely to assist the elaboration of structure–disease relationships. As mentioned above, covalently linked heterodimeric Gal-4 and Gal-8 prefer to aggregate suLac-presenting GDSs, while non-covalent homodimeric Gal-1 prefers Lac-presenting GDSs. This finding is identical to that of natural galectins in biology, and thus supports the hypothesis that GDSs are viable mimics of biological membranes that can help elucidate the structure and function of glycans. Moreover, the newly defined impacts on bridging activity revealed in the present work attest to the merit of this approach beyond this specific type of ligand and class of lectins. Thus, the present strategy of employing nanoscale GDSs—self-assembled from synthetic sulfatide mimics—to couple with natural and engineered lectins offers an opportunity to elucidate/deconstruct the subtlety of glycan–lectin interactions.

Methods

Preparation of GDSs. A stock solution was prepared by dissolving the required amount of amphiphilic JGDs in ethanol. GDSs were then generated by injection of 500 μL of the stock solution into 10 mL of PBS, followed by 5 s of vortexing.

Dynamic Light Scattering. Dynamic light scattering (DLS) measurements of GDSs were performed with a Malvern Zetasizer Nano-S instrument equipped with a 4-mW He–Ne laser (633 nm) and avalanche photodiode positioned at 175° to the beam. Instrument parameters and measurement times were determined automatically. Experiments were performed in triplicate.

Aggregation Assays. Aggregation assays of GDSs with lectins were monitored in semimicro disposable cuvettes (path length, l = 0.23 cm) at 23 °C at wavelength λ = 450 nm by using a Shimadzu UV-vis spectrophotometer UV-1601 with Shimadzu/UV Probe software in kinetic mode. PBS solution of galectin (100 μL) was injected into PBS solution of GDSs (900 μL). The cuvette was shaken by hand for 1 s to 2 s before data collection was started. The same GDSs solution was used as a reference. PBS solutions of galectin were prepared before the aggregation assays and were maintained at 0 °C (ice bath) before data collection.

ACKNOWLEDGMENTS. Inspiring discussions with Drs. B. Friday and A. Leddoz are acknowledged. Financial support from National Science Foundation Grants DMR-1066116 (to V.P.), DMR-1609556 (to D.A.H.), and DMR-1120901 (to D.A.H., M.L.K., and V.P.), the P. Roy Vagelos Chair at the University of Pennsylvania (V.P.), the European Union's Horizon 2020 research and innovation programme under the Marie Sklodowska-Curie Grant Agreement 642687 (to I.B.), the Science Foundation Ireland Grant 13/IA/1959 (to S.O.), and the Marie Curie Initial Training Network GLYCOPHARM Grant PITN-GA-2012-317297 (to S.O. and H.-J.G.) is gratefully acknowledged.

1. Bertozzi CR, Kiessling LL (2001) Chemical glycobiology. *Science* 291:2357–2364.
2. Kiessling LL, Splain RA (2010) Chemical approaches to glycobiology. *Annu Rev Biochem* 79:619–653.
3. Alley WR, Jr, Mann BF, Novotny MV (2013) High-sensitivity analytical approaches for the structural characterization of glycoproteins. *Chem Rev* 113:2668–2732.
4. Palaniappan KK, Bertozzi CR (2016) Chemical glycoproteomics. *Chem Rev* 116: 14277–14306.
5. Lee YC, Lee RT, eds (1994) *Neoglycoconjugates. Preparation and Applications* (Academic, San Diego).
6. Kiessling LL, Grim JC (2013) Glycopolymer probes of signal transduction. *Chem Soc Rev* 42:4476–4491.
7. Wesener DA, Dugan A, Kiessling LL (2017) Recognition of microbial glycans by soluble human lectins. *Curr Opin Struct Biol* 44:168–178.
8. Gabius H-J, Roth J (2017) An introduction to the sugar code. *Histochem Cell Biol* 147: 111–117.
9. Roy R, Murphy PV, Gabius H-J (2016) Multivalent carbohydrate-lectin interactions: How synthetic chemistry enables insights into nanometric recognition. *Molecules* 21: E629.
10. Hart GW (2013) Thematic minireview series on glycobiology and extracellular matrices: Glycan functions pervade biology at all levels. *J Biol Chem* 288:6903.
11. Gabius H-J, Manning JC, Kopitz J, André S, Kaltner H (2016) Sweet complementarity: The functional pairing of glycans with lectins. *Cell Mol Life Sci* 73:1989–2016.
12. Varki A (1997) Selectin ligands: Will the real ones please stand up? *J Clin Invest* 99: 158–162.
13. Vestweber D, Blanks JE (1999) Mechanisms that regulate the function of the selectins and their ligands. *Physiol Rev* 79:181–213.
14. Delbianco M, Bharate P, Varela-Aramburu S, Seeberger PH (2016) Carbohydrates in supramolecular chemistry. *Chem Rev* 116:1693–1752.
15. Kramer JR, Deming TJ (2010) Glycopolypeptides via living polymerization of glycosylated-L-lysine N-carboxyanhydrides. *J Am Chem Soc* 132:15068–15071.
16. Miura Y, Hoshino Y, Seto H (2016) Glycopolymer nanobiotechnology. *Chem Rev* 116: 1673–1692.
17. Schatz C, Lecommandoux S (2010) Polysaccharide-containing block copolymers: Synthesis, properties and applications of an emerging family of glycoconjugates. *Macromol Rapid Commun* 31:1664–1684.
18. Geng J, et al. (2007) Site-directed conjugation of "clicked" glycopolymers to form glycoprotein mimics: Binding to mammalian lectin and induction of immunological function. *J Am Chem Soc* 129:15156–15163.
19. Horan N, Yan L, Isobe H, Whitesides GM, Kahne D (1999) Nonstatistical binding of a protein to clustered carbohydrates. *Proc Natl Acad Sci USA* 96:11782–11786.
20. Polizzotti BD, Kiick KL (2006) Effects of polymer structure on the inhibition of cholera toxin by linear polypeptide-based glycopolymers. *Biomacromolecules* 7: 483–490.
21. Ruff Y, et al. (2010) Glycodynamers: Dynamic polymers bearing oligosaccharides residues–Generation, structure, physicochemical, component exchange, and lectin binding properties. *J Am Chem Soc* 132:2573–2584.
22. Munoz EM, Correa J, Riguera R, Fernandez-Megia E (2013) Real-time evaluation of binding mechanisms in multivalent interactions: A surface plasmon resonance kinetic approach. *J Am Chem Soc* 135:5966–5969.
23. Rabuka D, Forstner MB, Groves JT, Bertozzi CR (2008) Noncovalent cell surface engineering: Incorporation of bioactive synthetic glycopolymers into cellular membranes. *J Am Chem Soc* 130:5947–5953.
24. Belardi B, O'Donoghue GP, Smith AW, Groves JT, Bertozzi CR (2012) Investigating cell surface galectin-mediated cross-linking on glycoengineered cells. *J Am Chem Soc* 134:9549–9552.
25. Cook GMW (1986) Cell surface carbohydrates: Molecules in search of a function? *J Cell Sci Suppl* 4:45–70.
26. Gabius H-J (2017) How to crack the sugar code. *Folia Biol (Praha)* 63:121–131.
27. Ledeen RW, et al. (2012) Beyond glycoproteins as galectin counterreceptors: Tumor/effector T cell growth control via ganglioside GM1. *Ann NY Acad Sci* 1253:206–221.
28. Gabius H-J, ed (2009) *The Sugar Code. Fundamentals of Glycosciences* (Wiley-VCH, Weinheim, Germany).
29. Teichberg VI, Silman I, Beitsch DD, Resheff G (1975) A beta-D-galactoside binding protein from electric organ tissue of *Electrophorus electricus*. *Proc Natl Acad Sci USA* 72:1383–1387.
30. Sharon N (1994) When lectin meets oligosaccharide. *Nat Struct Biol* 1:843–845.
31. Barondes SH (1997) Galectins: A personal overview. *Trends Glycosci Glycotechnol* 9: 1–7.
32. Harrison FL, Chesterton CJ (1980) Factors mediating cell–cell recognition and adhesion. Galaptins, a recently discovered class of bridging molecules. *FEBS Lett* 122: 157–165.
33. Hirabayashi J (1997) Recent topics on galectins. *Trends Glycosci Glycotechnol* 9: 1–182.
34. Cooper DNW (2002) Galectinomics: Finding themes in complexity. *Biochim Biophys Acta* 1572:209–231.
35. Kaltner H, et al. (2017) Galectins: Their network and roles in immunity/tumor growth control. *Histochem Cell Biol* 147:239–256.
36. Percec V, et al. (2013) Modular synthesis of amphiphilic Janus glycodendrimers and their self-assembly into glycodendrimersomes and other complex architectures with bioactivity to biomedically relevant lectins. *J Am Chem Soc* 135:9055–9077.
37. Sherman SE, Xiao Q, Percec V (2017) Mimicking complex biological membranes and their programmable glycan ligands with dendrimersomes and glycodendrimersomes. *Chem Rev* 117:6538–6631.
38. Ahmad N, et al. (2004) Galectin-3 precipitates as a pentamer with synthetic multivalent carbohydrates and forms heterogeneous cross-linked complexes. *J Biol Chem* 279:10841–10847.
39. Allen HJ, Ahmed H, Matta KL (1998) Binding of synthetic sulfated ligands by human splenic galectin 1, a beta-galactoside-binding lectin. *Glycoconj J* 15:691–695.
40. Stowell SR, et al. (2008) Galectin-1, -2, and -3 exhibit differential recognition of sialylated glycans and blood group antigens. *J Biol Chem* 283:10109–10123.

41. Tu Z, et al. (2013) Synthesis and characterization of sulfated Gal-β-1,3/4-GlcNAc disaccharides through consecutive protection/glycosylation steps. *Chem Asian J* 8: 1536–1550.
42. Ideo H, Seko A, Ohkura T, Matta KL, Yamashita K (2002) High-affinity binding of recombinant human galectin-4 to SO(3)(-) → 3Galbeta1 → 3GalNAc pyranoside. *Glycobiology* 12:199–208.
43. Tateno H, et al. (2008) Glycoconjugate microarray based on an evanescent-field fluorescence-assisted detection principle for investigation of glycan-binding proteins. *Glycobiology* 18:789–798.
44. Roy R, et al. (2017) Teaming up synthetic chemistry and histochemistry for activity screening in galectin-directed inhibitor design. *Histochem Cell Biol* 147:285–301.
45. Ideo H, Seko A, Yamashita K (2005) Galectin-4 binds to sulfated glycosphingolipids and carcinoembryonic antigen in patches on the cell surface of human colon adenocarcinoma cells. *J Biol Chem* 280:4730–4737.
46. Vokhmyanina OA, et al. (2012) Comparative study of the glycan specificities of cell-bound human tandem-repeat-type galectin-4, -8 and -9. *Glycobiology* 22:1207–1217.
47. Bum-Erdene K, Leffler H, Nilsson UJ, Blanchard H (2015) Structural characterization of human galectin-4 C-terminal domain: Elucidating the molecular basis for recognition of glycosphingolipids, sulfated saccharides and blood group antigens. *FEBS J* 282:3348–3367.
48. Bum-Erdene K, Leffler H, Nilsson UJ, Blanchard H (2016) Structural characterisation of human galectin-4 N-terminal carbohydrate recognition domain in complex with glycerol, lactose, 3′-sulfo-lactose, and 2′-fucosyllactose. *Sci Rep* 6:20289.
49. Ideo H, Seko A, Ishizuka I, Yamashita K (2003) The N-terminal carbohydrate recognition domain of galectin-8 recognizes specific glycosphingolipids with high affinity. *Glycobiology* 13:713–723.
50. Carlsson S, et al. (2007) Affinity of galectin-8 and its carbohydrate recognition domains for ligands in solution and at the cell surface. *Glycobiology* 17:663–676.
51. Stowell SR, et al. (2008) Dimeric galectin-8 induces phosphatidylserine exposure in leukocytes through polylactosamine recognition by the C-terminal domain. *J Biol Chem* 283:20547–20559.
52. Hirabayashi J, et al. (2002) Oligosaccharide specificity of galectins: A search by frontal affinity chromatography. *Biochim Biophys Acta* 1572:232–254.
53. Chien CH, Ho M-R, Lin C-H, Hsu SD (2017) Lactose binding induces opposing dynamics changes in human galectins revealed by NMR-based hydrogen-deuterium exchange. *Molecules* 22:E1357.
54. Percec V, et al. (2010) Self-assembly of Janus dendrimers into uniform dendrimersomes and other complex architectures. *Science* 328:1009–1014.
55. Peterca M, Percec V, Leowanawat P, Bertin A (2011) Predicting the size and properties of dendrimersomes from the lamellar structure of their amphiphilic Janus dendrimers. *J Am Chem Soc* 133:20507–20520.
56. Xiao Q, et al. (2016) Self-sorting and coassembly of fluorinated, hydrogenated, and hybrid Janus dendrimers into dendrimersomes. *J Am Chem Soc* 138:12655–12663.
57. Xiao Q, et al. (2016) Bioactive cell-like hybrids coassembled from (glyco)dendrimersomes with bacterial membranes. *Proc Natl Acad Sci USA* 113:E1134–E1141.
58. Xiao Q, et al. (2017) Janus dendrimersomes coassembled from fluorinated, hydrogenated, and hybrid Janus dendrimers as models for cell fusion and fission. *Proc Natl Acad Sci USA* 114:E7045–E7053.
59. Zhang S, et al. (2014) Mimicking biological membranes with programmable glycan ligands self-assembled from amphiphilic Janus glycodendrimers. *Angew Chem Int Ed Engl* 53:10899–10903.
60. Zhang S, et al. (2015) Dissecting molecular aspects of cell interactions using glycodendrimersomes with programmable glycan presentation and engineered human lectins. *Angew Chem Int Ed Engl* 54:4036–4040.
61. Zhang S, et al. (2015) Unraveling functional significance of natural variations of a human galectin by glycodendrimersomes with programmable glycan surface. *Proc Natl Acad Sci USA* 112:5585–5590.
62. Kopitz J, et al. (2017) Reaction of a programmable glycan presentation of glycodendrimersomes and cells with engineered human lectins to show the sugar functionality of the cell surface. *Angew Chem Int Ed Engl* 56:14677–14681.
63. Zhang S, et al. (2015) Glycodendrimersomes from sequence-defined Janus glycodendrimers reveal high activity and sensor capacity for the agglutination by natural variants of human lectins. *J Am Chem Soc* 137:13334–13344.
64. Xiao Q, et al. (2016) Onion-like glycodendrimersomes from sequence-defined Janus glycodendrimers and influence of architecture on reactivity to a lectin. *Proc Natl Acad Sci USA* 113:1162–1167.
65. Xiao Q, et al. (2016) Why do membranes of some unhealthy cells adopt a cubic architecture? *ACS Cent Sci* 2:943–953.
66. Guilbert B, Davis NJ, Flitsch SL (1994) Regioselective sulfation of disaccharides using dibutylstannylene acetals. *Tetrahedron Lett* 35:6563–6566.
67. Braccia A, et al. (2003) Microvillar membrane microdomains exist at physiological temperature. Role of galectin-4 as lipid raft stabilizer revealed by "superrafts." *J Biol Chem* 278:15679–15684.
68. Wu AM, et al. (2004) Effects of polyvalency of glycotopes and natural modifications of human blood group ABH/Lewis sugars at the Galbeta1-terminated core saccharides on the binding of domain-I of recombinant tandem-repeat-type galectin-4 from rat gastrointestinal tract (G4-N). *Biochimie* 86:317–326.
69. Delacour D, et al. (2005) Galectin-4 and sulfatides in apical membrane trafficking in enterocyte-like cells. *J Cell Biol* 169:491–501.
70. Stechly L, et al. (2009) Galectin-4-regulated delivery of glycoproteins to the brush border membrane of enterocyte-like cells. *Traffic* 10:438–450.
71. Velasco S, et al. (2013) Neuronal galectin-4 is required for axon growth and for the organization of axonal membrane L1 delivery and clustering. *J Neurochem* 125:49–62.
72. Kopitz J, Ballikaya S, André S, Gabius H-J (2012) Ganglioside GM1/galectin-dependent growth regulation in human neuroblastoma cells: Special properties of bivalent galectin-4 and significance of linker length for ligand selection. *Neurochem Res* 37:1267–1276.
73. Rustiguel JK, et al. (2016) Full-length model of the human galectin-4 and insights into dynamics of inter-domain communication. *Sci Rep* 6:33633.
74. Göhler A, et al. (2010) Hydrodynamic properties of human adhesion/growth-regulatory galectins studied by fluorescence correlation spectroscopy. *Biophys J* 98:3044–3053.
75. Su ZZ, et al. (1996) Surface-epitope masking and expression cloning identifies the human prostate carcinoma tumor antigen gene PCTA-1 a member of the galectin gene family. *Proc Natl Acad Sci USA* 93:7252–7257.
76. Gentilini LD, et al. (2017) Stable and high expression of galectin-8 tightly controls metastatic progression of prostate cancer. *Oncotarget* 8:44654–44668.
77. Zick Y, et al. (2002) Role of galectin-8 as a modulator of cell adhesion and cell growth. *Glycoconj J* 19:517–526.
78. Tsai C-M, et al. (2011) Galectin-1 and galectin-8 have redundant roles in promoting plasma cell formation. *J Immunol* 187:1643–1652.
79. Tribulatti MV, Figini MG, Carabelli J, Cattaneo V, Campetella O (2012) Redundant and antagonistic functions of galectin-1, -3, and -8 in the elicitation of T cell responses. *J Immunol* 188:2991–2999.
80. Friedel M, André S, Goldschmidt H, Gabius H-J, Schwartz-Albiez R (2016) Galectin-8 enhances adhesion of multiple myeloma cells to vascular endothelium and is an adverse prognostic factor. *Glycobiology* 26:1048–1058.
81. Kaltner H, et al. (2009) Unique chicken tandem-repeat-type galectin: Implications of alternative splicing and a distinct expression profile compared to those of the three proto-type proteins. *Biochemistry* 48:4403–4416.
82. Pál Z, et al. (2012) Non-synonymous single nucleotide polymorphisms in genes for immunoregulatory galectins: Association of galectin-8 (F19Y) occurrence with autoimmune diseases in a Caucasian population. *Biochim Biophys Acta* 1820:1512–1518.
83. Ruiz FM, et al. (2014) Natural single amino acid polymorphism (F19Y) in human galectin-8: Detection of structural alterations and increased growth-regulatory activity on tumor cells. *FEBS J* 281:1446–1464.
84. Levy Y, et al. (2006) It depends on the hinge: A structure-functional analysis of galectin-8, a tandem-repeat type lectin. *Glycobiology* 16:463–476.
85. Wang J, et al. (2009) Cross-linking of GM1 ganglioside by galectin-1 mediates regulatory T cell activity involving TRPC5 channel activation: Possible role in suppressing experimental autoimmune encephalomyelitis. *J Immunol* 182:4036–4045.
86. Amano M, et al. (2012) Tumour suppressor p16(^{INK4a})–Anoikis-favouring decrease in N/O-glycan/cell surface sialylation by down-regulation of enzymes in sialic acid biosynthesis in tandem in a pancreatic carcinoma model. *FEBS J* 279:4062–4080.
87. Romaniuk MA, et al. (2010) Human platelets express and are activated by galectin-8. *Biochem J* 432:535–547.
88. Nishi N, Itoh A, Shoji H, Miyanaka H, Nakamura T (2006) Galectin-8 and galectin-9 are novel substrates for thrombin. *Glycobiology* 16:15C–20C.
89. Weinmann D, et al. (2016) Galectin-3 induces a pro-degradative/inflammatory gene signature in human chondrocytes, teaming up with galectin-1 in osteoarthritis pathogenesis. *Sci Rep* 6:39112.
90. Toegel S, et al. (2014) Human osteoarthritic knee cartilage: Fingerprinting of adhesion/growth-regulatory galectins *in vitro* and *in situ* indicates differential up-regulation in severe degeneration. *Histochem Cell Biol* 142:373–388.
91. Kopitz J, et al. (2001) Negative regulation of neuroblastoma cell growth by carbohydrate-dependent surface binding of galectin-1 and functional divergence from galectin-3. *J Biol Chem* 276:35917–35923.
92. Sanchez-Ruderisch H, et al. (2010) Tumor suppressor p16 ^{INK4a}: Downregulation of galectin-3, an endogenous competitor of the pro-anoikis effector galectin-1, in a pancreatic carcinoma model. *FEBS J* 277:3552–3563.
93. Nieminen J, Kuno A, Hirabayashi J, Sato S (2007) Visualization of galectin-3 oligomerization on the surface of neutrophils and endothelial cells using fluorescence resonance energy transfer. *J Biol Chem* 282:1374–1383.
94. Rao TD, et al. (2017) Antibodies against specific MUC16 glycosylation sites inhibit ovarian cancer growth. *ACS Chem Biol* 12:2085–2096.
95. Kopitz J, et al. (2014) Human chimera-type galectin-3: Defining the critical tail length for high-affinity glycoprotein/cell surface binding and functional competition with galectin-1 in neuroblastoma cell growth regulation. *Biochimie* 104:90–99.
96. Ideo H, Matsuzaka T, Nonaka T, Seko A, Yamashita K (2011) Galectin-8-N-domain recognition mechanism for sialylated and sulfated glycans. *J Biol Chem* 286: 11346–11355.
97. Yang RY, Hill PN, Hsu DK, Liu FT (1998) Role of the carboxyl-terminal lectin domain in self-association of galectin-3. *Biochemistry* 37:4086–4092.
98. Halimi H, et al. (2014) Glycan dependence of galectin-3 self-association properties. *PLoS One* 9:e111836.
99. Ippel H, et al. (2016) Intra- and intermolecular interactions of human galectin-3: Assessment by full-assignment-based NMR. *Glycobiology* 26:888–903.
100. Manning JC, et al. (2017) Lectins: A primer for histochemists and cell biologists. *Histochem Cell Biol* 147:199–222.
101. Nishimura S (2011) Toward automated glycan analysis. *Adv Carbohydr Chem Biochem* 65:219–271.
102. Shimoda A, Tahara Y, Sawada S-I, Sasaki Y, Akiyoshi K (2017) Glycan profiling analysis using evanescent-field fluorescence-assisted lectin array: Importance of sugar recognition for cellular uptake of exosomes from mesenchymal stem cells. *Biochem Biophys Res Commun* 491:701–707.
103. Batista BS, Eng WS, Pilobello KT, Hendricks-Muñoz KD, Mahal LK (2011) Identification of a conserved glycan signature for microvesicles. *J Proteome Res* 10:4624–4633.
104. Gomes J, et al. (2015) Extracellular vesicles from ovarian carcinoma cells display specific glycosignatures. *Biomolecules* 5:1741–1761.